Northern States Power Company

414 Nicollet Mall
Minneapolis, Minnesota 55401
Telephone (612) 330-5500

September 29, 1987

Director
Office of Nuclear Reactor Regulation
US Nuclear Regulatory Commission
Attn: Document Control Desk
Washington DC 20555

PRAIRIE ISLAND NUCLEAR GENERATING PLANT
Docket Nos. 50-282 License Nos. DPR-42
50-306 DPR-60

Additional Information to Support the
Submittal of NSPNAD-8608 and NSPNAD-8609

This submittal is responding to an August 5, 1987 NRC Staff request for additional information related to the submittal of NSPNAD-8608 and NSPNAD-8609. This information was requested to be submitted by September 14, 1987. A two week extension was requested and granted from the NRC Monticello Project Manager. A copy of this submittal and selected references will be express mailed to the NRC subcontract reviewers.

Please contact us if you have any questions related to the information we have provided.

David Musolf
Manager - Nuclear Support Services

c: Regional Administrator III, NRC
Sr NRR Project Manager, NRC
Sr Resident Inspector, NRC
G Charnoff
State of Minnesota
Attn: Dr J W Ferman
Brookhaven National Laboratory

Attachments:

Response to NRC Questions on the NSP Reactor Physics Methods Qualification for Monticello - NSPNAD-8609

Response to NRC Questions on the NSP Reload Safety Evaluation Methods for Monticello - NSPNAD-8608

A001
1/1

Response to NRC Questions on the NSP Reactor Physics Methods Qualification
for Monticello
NSPNAD-8609

Question 1

In order to eliminate selected TIP readings from the statistical analysis, it should be demonstrated that the eliminated TIP signals are in fact erroneous and are not, in fact, a result of differences between the design model and the as-built core. What is the increase in the reliability factors when no TIP signals are eliminated?

Response

The uncertainty should not contain the differences between the as-built core and the model. The uncertainty should contain only the differences between the known core and the modelling of that core. This uncertainty includes calculational uncertainty and measurement uncertainties (including material tolerances) but not misplaced bundles or mispositioned detector tubes. The resultant model will then be used to design future cores that we expect to operate within an uncertainty band that we have determined from the above process. The plant monitoring function is then used to monitor all tip traces to assure tech-spec compliance.

As an example of this logic, if a bundle is misplaced in a monitored location in the core then the monitoring function will identify this as a major difference between predicted and measured results. This major difference should not be included in the model uncertainty data base for the next cycle since it would give a very conservative and unrealistically high value.

The purpose of the qualification process is to separate the uncertainties derived from TIP misalignment from the total of calculational plus measurement uncertainty. The following calculation demonstrates that this approach gives conservative results compared to the classic approach of subtracting measurement uncertainty from total uncertainty and reporting only calculational uncertainty.

By examining the statistics of the symmetric subset of the database (A-sequence and all rods out statepoints) we can estimate the measurement uncertainty of the total database. For this subset of the data, the measured asymmetry (difference in measurements between sets of TIPs across the line of symmetry) has a standard deviation of 6.111%, whereas the predicted asymmetry has a standard deviation of .838% For this same case the standard deviation of measured minus predicted differences is 5.269%. Via reference #1 it is concluded that measurement uncertainty is approximately one half of the measured asymmetry. So that the calculational uncertainty (σ(cal)) is

$$\sigma(cal) = [(\sigma(m-p))^{**}2 - ((\sigma(m-m)/2)^{**}2)]^{\frac{1}{2}}$$

with

$\sigma(m-p)$ = 5.27% = standard deviation of measured-predicted difference
$\sigma(m-m)$ = 6.11% = standard deviation of measured-measured difference (calculated across the core line of symmetry)

we see that

$\sigma(cal)$ = 4.30% = calculational uncertainty

The value stated in the topical for total uncertainty is 4.70%. Thus, this alternative approach demonstrates that the method used in the topical produces a conservative uncertainty, hence a conservative RF.

However, if one neither subtracts measurement uncertainty nor removes highly suspect TIPs from the data base then the APLHGR and LHGR reliability factors (R.F.s) would be 12.3% up from 11.1% in the Topical. The MCPR R.F. would be 9.5%, up from 8.1%.

Reference

1. EPRI Report NP-1278, "Online Nuclear Power Distribution Measurement," Appendix A.

Question 2

Describe in detail how the value $\%\Delta K/\%\Delta V$ = .0077 is determined from the data in Table 3.3.1.

Response

By taking the change in k-effective between the first and last entry for each cycle and dividing that ΔK by the associated ΔV, one can produce a $\Delta K/\Delta V$ for each cycle (cycle 7 has a zero term). The first and last entries were used to get a larger difference and thereby minimize measurement error. By averaging these values we get: $\%\Delta K/\%\Delta V$ (4 cycle average) = .0077.

Question 3

Provide quantitative justification (using results from references 5-8 if appropriate) that the 95/95 upper tolerance limit on the Doppler coefficient is RF_{DOP} = .10.

Response

The traditional industry approach to Doppler uncertainty has been to select a value based on engineering judgement and then to provide qualitative justification for the value, usually based on Resonance Integral Comparison with references 5-8 as the bases. The 10% value quoted in the topical was based on what was judged to be "industry acceptance accuracies". After a re-review of references 5-8, it is concluded that there is no data contained in those documents to quantitatively support a 10%, 95/95 upper tolerance limit on the Doppler coefficient. Further, it is believed that little data exists in the industry that would provide a quantitative justification for a 10% reliability action, particularly for a BWR.

The calculation of Doppler for a reactor core has two main components; 1) the calculation of Doppler reactivity associated with the average fuel temperature and selected voids, by one of the cross sections generator codes; 2) the calculation of nodal fuel temperature and voids throughout the core, and the spatial weighting of the Doppler reactivity associated with each node by one of the nodal codes. The accuracy of the calculation of Doppler reactivity for a core is a function of both components.

There are few meaningful power coefficient measurement results that exist, and those that do are from PWRs hence, as stated, there is little measured data available that could be used to provide a quantitative justification for a 10% reliability factor for the calculational results from the two components.

Preliminary results from a study currently underway by EPRI indicate that the Doppler reactivity as calculated by a number of cross section generator codes shows differences greater than 10%. Which code is the "more correct" nas not yet been determined. Based on this and the aforementioned lack of reactor measurement, it is our engineering judgement that a 25% reliability factor be used with the Monticello Doppler reactivity for the near future. When, and if the difference between the cross section generator codes are resolved and a "correct" one identified, the uncertainty for the NSP Doppler model will be readdressed.

Questions 4, 8, and 9

These three questions will be addressed together to better clarify the relationship of the normalization factors.

Question 4

The NDH model has been normalized to the Monticello cycles 7 through 10 measurement data and, consequently, the reliability factors determined from the cycle 7-10 calculation/measurement differences are smaller than those for a cycle to which NDH has not been normalized. What increase in the reliability factors is expected for future cycles and how is this accounted for?

Question 8

Are the generic normalization factors based on data from cycles 7 through 10? Are these factors intended for use in all future cycles of Monticello? What core parameters affect these rormalization factors? How are these factors affected by operating history?

Question 9

Describe the methods used to generate the radial albedos and leakage factors. How is void dependence in the radial albedos determined? Are these albedos updated for each cycle? How sensitive are the albedos to exposure, rod pattern, temperature and core loading?

Response

The normalization of the Monticello nodal model consists of two distinct parts; the normalization of certain parameters to plant measurements and a generic normalization to ¼ core PDQ7 models. The parameters adjusted in the normalization to plant measurements included vertical and horizontal albedos or leakage factors and vertical and horizontal Kernel mixing factors. A different set of albedos and mixing factors is used for normal operating conditions than for cold shutdown conditions since separate NDH models exist for hot and cold conditions. Values for the hot NDH model were determined from comparisons to cycles 5 and 6 plant data and were then used without alteration for the cycles 7-10 database. Values for the cold model were determined from comparisons to cycles 7 through 10 plant data. The generic normalization to quarter core depleted PDQ7 models was done at 0%, 40%, and 70% void for cycles 5 and 6 and at 40% void for cycle 7. The albedos, mixing factors, and generic PDQ7 factors were used for the entire cycles 7-10 database and will be used without alteration for all future Monticello cycles.

Based on the method used to determine these parameters, the reliability factors are not expected to increase for future cycles. All reliability factors will be re-evaluated via procedure at the end of each cycle to ensure that they are still valid. As an example look at power distribution.

The power distribution reliability factors for a specific cycle will be calculated by comparing predicted to measured reaction rates from the three most recent previously completed cycles. This three cycle running database allows us to follow trends more quickly and keeps the size of the database manageable. For example: Monticello cycle 13 would use reaction rates from cycles 9, 10, and 11. Cycle 12 reaction rates are not included in this update because cycle 12 would not be complete.

If a cycle's reliability factors should show an increase from those presented in the topical, the higher reliability factors will be used for safety related calculations. The updated reliability factors will be presented in the Reload Safety Evaluation for the cycle in question.

The power distribution statistics methods follow those presented in the Prairie Island Topical (Reference 2). In the Prairie Island methodology it was determined that three previous cycles of measured to predicted reaction rates would be sufficient to determine updated power distribution reliability factors. This same criterion will be used at Monticello.

The void dependence of the radial albedos is handled by the following correlation.

$$\alpha_{ijk} = AH_{ij} * [1 + 0.95 (V_{ijk} - 0.4)]$$

where

α_{ijk} = radial albedo applied to node ijk

AH_{ij} = input value derived from normalization process

V_{ijk} = node ijk void fraction

0.95 and 0.4 = correlation constants from Reference 3

Reference 3 (page 4.5 and Appendix E) describes the derivation of the void dependent albedo correlation. The correlation constants were derived as part of the work in Reference 3 and were confirmed to be valid for Monticello via PDQ7 quarter core calculations at three void levels.

The sensitivities of the various parameters are as follows.

The generic PDQ7 factors have been determined to be a function of core location and have shown slight, if any, dependence on various other core parameters including operating history.

For the albedos and mixing factors the NDH methodology accounts for the change in nodal neutronic properties due to exposure, temperature (voids) and rod presence and for the change in coupling between nodes due to rod patterns and core loading. As previously stated, a different set of albedos and mixing factors accounts for the differences between hot operating conditions and cold shutdown.

References

2. "Qualification of Reactor Physics Methods for Application to Prairie Island," NSPNAD-8101 Revision 1, December 1982.

3. "Technical Description and Evaluation of BWR Hybrid Power Shape Monitoring System," EPRI NP-2234, March 1982.

Question 5

In view of the differences between the PWR and BWR measurement systems and the sources of the measurement system errors, demonstrate the factor of three reduction in the number of measurements is adequate to account for the lack of independence of the Monticello measurement errors.

Response

Examination of the respective measurement systems brings one to the conclusion that they are in fact very similar, and one would expect similar correlation of the data.

The calculation used to determine the reduction factor of three was reviewed and it was decided that a factor of ten should be used for conservatism. Applying this factor raises the APLHGR and LHGR reliability factor to .113, up from .111. This indicates that the reliability factors are relatively insensitive to the reduction factor used. The topical will be revised to reflect this change.

Question 6

In the calculation of both the void coefficient and control rod worth reliability factors, the error in the void and control rod reactivity defects, $\delta\Delta\rho$, is assumed to be the same as the error in the statepoint k_{eff}, δk_{eff}. In fact, in the determination of the reactivity defect, $\Delta k = k_{eff,2} - k_{eff,1}$, the statepoint error, δk_{eff}, to a good approximation, "subtracts out" and the reactivity defect error, $\delta\Delta k$, is independent of the statepoint error, δk_{eff}. Therefore, provide a calculation of the void coefficient and control rod worth reliability factors based on the error in predicting the void and control rod reactivity differences.

Response

As stated in the topical, the void coefficient and the total control rod worth cannot be directly measured in a BWR and hence the error in predicting void and control rod reactivity differences must be determined qualitatively.

Ideally, if one had a series of statepoints where only one state parameter varied, e.g., void, then the variation in the calculated k_{eff} of these statepoints could be attributed to the error or uncertainty in the void and/or void reactivity prediction. The statepoint error "subtracts out" only if the error is constant for all statepoints, i.e., it is a bias and as such would be reflected in the mean k_{eff} and not in the uncertainty about the mean.

As an example, the data in Table 3.6.1 for the 100% power statepoints yields -

Mean k_{eff} = .9911 ± .0017

The bias is 0.0089Δρ, the uncertainty is ± 0.0017. For these statepoints, xenon, Doppler and void are relatively constant. Hence, they contribute to the bias, but not necessarily to the uncertainty. The uncertainty is attributable to what is varying, which is exposure, rod density and measurement.

Similarly, the data in Table 3.3.1 has statepoints where xenon, Doppler and void are also changing. The uncertainty in these statepoints includes the error in these parameters as well as exposure and measurement. How much of the uncertainty that is attributable to each parameter cannot be determined. As a point of interest, the uncertainty for these coastdown points, where void, Doppler and xenon are varying, is about the same as for the total data base where they are nearly constant (Section 4.1.3), which indicates their contribution to the uncertainty is small.

Table 3.3.2 presents data from a cycle 7 pump trip. Here, only Doppler, void and xenon are varying, hence the uncertainty is due to these parameters and measurement. This uncertainty is smaller than for the total 100% power data base and smaller than the uncertainty from just the Cycle 7 100% power statepoints, again indicating the contribution to the uncertainty from the parameter of interest, void, is small.

Because the uncertainty components are not separable and based on the above rationale that the contribution from voids must be small, the total uncertainty associated with the statepoints in Table 3.3.1 was assumed to be from voids, and a value inferred for voids alone.

A similar rationale can be made for rod worth uncertainty. Table 3.1.1 lists a number of statepoints for the ambient temperature (i.e., cold) conditions. The variables contributing to the uncertainty in calculating k_{eff} are rod worth, exposure, temperature effects and measurement error, the largest contributors being the first two.

The reactivity being held down in the cores in Table 3.1.1 ranges from 8.0% to 8.9% Δρ. In order for the bias to be zero, i.e., the mean k_{eff} ~ 1.0, either the rod worth and exposure worth are being calculated very close to actual, or they are compensating almost exactly. For example, if the exposure worth were being calculated correctly and rod worth was low by 10%, the mean k_{eff} would be ~1.008,

and vice versa. However, if the exposure reactivity error were just compensating for rod worth error in the cold cases, the same exposure error would also have to be just compensating for other effects (ie. xenon, Doppler, void) during coastdown, which seems an unlikely coincidence.
A number of qualitative points can be made from the data in Table 3.1.1.

1. Rod worth vs exposure is being calculated correctly since there is no drift in the calculated k_{eff} with average core exposure.

2. The spatial distribution of flux is being calculated correctly since the local criticals (large local gradients) and in sequence criticals (more uniformly distributed flux) are being calculated to the same accuracy within a cycle.

3. The rod density variation from cycle to cycle and within a cycle has no noticeable effect on the calculated k_{eff}.

Based on the above rationales, the total uncertainty in the calculated k_{eff} of Table 3.1.1 was attributed to rod worth error.

This rationale demonstrates the validity of the void coefficient and rod worth reliability factors. In addition, the values quoted for these reliability factors are consistent with industry accepted values.

Question 7

Based on the comparisons of Table 3.6.3 and Figure 3.6.44 it is concluded that all γ-scan measurement data was not included in the power distribution comparisons. On what basis was the measured data discarded and what effect does this data selection have on the reliability factors?

Response

Table 3.6.3 was included to show representative data for the power distribution comparisons and does not include the entire database. All of the gamma scan measurement data was included in the determination of the reliability factors, none was discarded.

Question 10

Describe the procedure used to derive the correction factor for a bundle moved from a peripheral to a central location. How sensitive is this correction factor to exposure, rod pattern, temperature, and core loading?

Response

The peripheral correction factors were generated in the following way. Nodal ¼ core NDH k-infinities were normalized to ¼ core PDQ k-infinities at 2000 hrs and 4000 hrs at 40% void conditions in cycle 6. The normalization factors (unrodded and rodded k-infinite multipliers, XKN and XKR) from the 40% void case were used in 0% and 70% void normalization cases to check the void dependence of the generic factors. From these 0% and 70% void normalizations, it was clear that using only 40% void based XKNs and XKRs was not adequate for bundles on the periphery in past cycles; an additional correction was required.

For instance, a normalization at 0% void was run at 2000 hrs into cycle 6 with XKN and XKR arrays input from a 40% void normalization case. A new set of k-infinite multipliers was then calculated for 0% void conditions. The mean of the k-infinite multipliers was significantly different from unity for bundles that were on the periphery in cycle 5 and were moved to the interior in cycle 6. The same procedure was followed at 70% void and at 4000 hrs at both voids. A normalization was then run at 40% void conditions in cycle 7 to validate the correction.

Based on the cycles 6 and 7 data very little exposure or core loading dependence was noted for this correction.

The effect of rod presence is accounted for directly because the correction factors are specific for unrodded and rodded nodes. The rodded k-infinite multipliers came from rodded PDQ to nodal comparisons as described above. Comparisons of XKN at 2000 and 4000 hours for four rod sequences were made. The dependence of the unrodded correction factor on the rod sequence was small.

This correction is used in both the hot and the cold NDH models. Since the same correction is used in both models and statepoint comparisons in the topical show very good agreement at both temperatures, it is concluded that temperature dependence is insignificant. Due to the current low leakage loading strategy, the last cycle to have bundles shuffled from the periphery to the interior was cycle 9.

Question 11

Describe the spectrum correction factor used to correct for the extrapolated flux.

Response

The spectrum correction factor (SCF) used in NDH is calculated by the following correlation.

$$SCF = 1.08 + 0.17 * V$$

where

V = nodal void fraction
1.08 and 0.17 = correlation constants from Reference 4

The SCF is applied in the NDH source to power to source transformations for edge nodes by the following equation.

$$P = S * SCF * KFNUF$$

where

S = nodal source value
P = nodal power value
KFNUF = nodal $K\Sigma_f/\nu\Sigma_f$

The derivation of the SCF is described in Reference 4 (Appendix E).

Reference

4. "Technical Description and Evaluation of BWR Hybrid Power Shape Monitoring System," EPRI NP-2234, March 1982.

Question 12

How are incore detector signals calculated? Specifically, indicate how the contributions from each of four dissimilar uncontrolled/controlled assemblies are derived, indicating the parameter dependence.

Response

The predicted incore detector signals are calculated by the SGM program from the power, void, and exposure distributions predicted by NDH and the input instrument factors. The calculated incore detector signal reflects contributions of the four surrounding bundles.

$$\text{SENSOR READING} = \sum_{4} P_{ijk} * IF_{ijk}$$

where

$$IF_{ijk} = CO(NFT,IY) + C1(NFT,IY) * E + C2(NFT,IY) * E^2 + C3(NFT,IY) * E^3 + C4(NFT,IY) * E^4 + (C5(NFT,IY) + C6(NFT,IY) * E + C7(NFT,IY) * E^2)\ (1-U/U\ Base)$$

Each bundle's contribution is calculated from the NDH nodal power multiplied by the input instrument factor for that bundle. The instrument factors are functions of fuel type (NFT), location (ijk), nodal void (U), nodal exposure (E), and the control rod configuration (IY) of the four bundles surrounding the detector. C0-C7 are constants and P is the nodal power. The instrument factors are obtained from CASMO with generic normalization corrections from quarter core PDQ-7 models of cycles 5, 6, and 7 to account for flux gradients caused by position relative to the core periphery and the control rod configurations.

Question 13

Do any of the few-rod criticals listed in Table 3.1.1 include the withdrawal of the highest worth (strongest) rod at the time the critical was measured? If not, how would this withdrawal effect the results of the measurement/calculation comparisons?

Response

Table 4.1.1 indicates which of the criticals listed in Table 3.1.1 are few rod criticals and which are in-sequence criticals. In cycles 7, 9, and 10 the criticals were pulled around the highest worth predicted rod. In cycle 8 the first critical listed was pulled around the high worth rod while the other two few rod criticals were pulled in the vicinity of test assemblies.

For each high worth rod critical, the high worth rod was fully withdrawn first and then diagonally adjacent rods were pulled in order until criticality was achieved. This gives a good comparison of the measured to calculated high worth rod. In the remaining two criticals, face adjacent rods were withdrawn.

The measurement/calculation comparisons would not be affected by exclusion of the highest worth rod. This is indicated by the data in Table 3.1.1.

Question 14

How are uncertainties in the fuel pin temperature associated with power changes accounted for in the Doppler reliability factor? Similarly, how are uncertainties resulting from differences between the as-built and assumed dimensions and/or materials and fuel densification treated?

Response

The Doppler coefficient for the reactor is calculated from a three dimensional nodal model where the change in Doppler reactivity at each node is calculated and incorporated into the spatial flux calculation. The nodal Doppler reactivity change is calculated from the nodal fuel temperature change. Hence, the relationship of importance is between the ΔT_{fuel} and the resultant change in Doppler reactivity during a transient.

The change in Doppler reactivity is proportional to the difference of the square root of the fuel temperatures, i.e.,

$$\rho_{T_{fuel\ 1}} - \rho_{T_{fuel\ 2}} \propto (T_{fuel\ 1})^{\frac{1}{2}} - (T_{fuel\ 2})^{\frac{1}{2}}$$

The uncertainties in absolute fuel temperature of a node, be they from variations in as built dimensions and/or materials, fuel densification or whatever, principally impact the base fuel temperature and Doppler defect, and only secondarily the Doppler coefficient. For example, assume that the calculated nodal fuel temperature is 1200 °F and the associated Doppler reactivity is 0.010 $\Delta\rho$ (550 °F to 1200 °F), and assume the calculated nodal fuel temperature during a transient changes by 500 °F (1200 °F to 1700 °F). The reactivity calculated from this fuel temperature change by the nodal representation is 0.0064 $\Delta\rho$

Now, assume the actual nodal fuel temperature is 1100 °F and the change in fuel temperature is also 500 °F (since transients where Doppler is important, e.g., rod drop, are over in seconds the transient is nearly an adiabatic process and the node will undergo approximately the same ΔT independent of the base temperature). The reactivity associated with the nodal fuel temperature change is 0.0066$\Delta\rho$, about 3% larger than using 1200 °F as the base fuel temperature.

It is probable that dimensions and material variations (due to tolerances, etc.) would be such that the effects would cause both higher and lower temperatures than calculated using nominal dimensions, and hence the overall effect on the core would be smaller than that estimated above. Therefore, no attempt is made to include these effects.

In addition the Doppler coefficient has only a small effect on the calculation of the core energy release and hence the response for the design basis transient.

Question 15

What effect do the differences (e.g. cross sections) between versions of CASMO used in the Kritz benchmarking and the more recent version used by NSP (CASMO-II) have on the reliability factors?

Response

NSP departs somewhat from standard practice by using the EPRI-CPM production library in CASMO for Monticello, rather than the library supplied by Studsvik. The differences between the CPM, CASMO-I, and CASMO-II libraries are minor with one exception, and should not, by their nature affect the benchmarking. The exception is a difference in the size of the lumped fission product absorption cross-sections, the values in CPM being twice as large. This difference is why NSP uses the CPM library, producing a somewhat flatter eigen-value with exposure. Since the effect of this is already in our hot and cold critical comparisons, our stated uncertainties include it. This library is the same as used in the EPRI benchmarking for CPM in the ARMP documentation. Additionally, via Reference 5 it is concluded that the CASMO-I and CASMO-II libraries, for all practical purposes, are identical.

Returning to the question of the Kritz data, the earliest benchmarking of Doppler was completed with a version of the CASMO library that predates all of the current versions, although the differences are also not overly large. Again through Reference 5, the primary difference is in the resonance absorption in U-238. The following factor was applied (Reference 6).

$$\sigma^{238'}_{a,g} = \sigma^{238}_{a,g} * .30\ [1-RI/\tau\sigma_p]^2 \text{ for groups between 15 and 27 of 69}$$

In regard to our reliability factors, all factors use the Kritz benchmarking only as additional supportive information, hence the RF would not be affected by minor cross section changes. The Doppler RF is expanded on in question 3.

References

5. Tele-con with Malte Edenius of Studsvik of America Co-Author of CASMO, CPM and numerous industry papers, August 31, 1987.

6. Studsvik Report "CASMO, the Data Library," Studsvik/K2-81/491, March 19, 1981.

Question 16

Are control rod history effects accounted for in the NDH calculations and, if not, how are the uncertainties introduced by this simplification accounted for?

Response

Control rod history effects are modelled explicitly in the NDH nodal code. These effects are calculated by the CASMO-II computer code and are input for each fuel type. Reference 7 (Section 2.2.2.5) describes the methods used to model this effect.

Reference

7. NSP NDH User Manual, version NDH85047, 1985.

Question 17

Has the effect of excluding from consideration 8 of the 48 axial values of the instrument signals been evaluated? What is the increase in the uncertainty and, correspondingly, what is the additional allowance by which the power distribution reliability factor must be increased when this data is not excluded?

Response

The effect of excluding the top and bottom 4 axial values from consideration in the data base has been considered. Also the different nature of the measurement uncertainty in this region has been considered. Different nature means that measurement uncertainty is a stronger function of axial misalingnment due to the steep flux gradient in this region, whereas in the core center, uncertainty comes more from radial misalignment. Since the peak power can never occur in the excluded region it was concluded that although the errors appear quite large, practically speaking they are not significant. It is also important to realize that the top and bottom 6 inches (2 axial levels) of the fuel are natural uranium blankets. However, when these nodes are included in the data base the resultant uncertainty and reliability factors are

	Topical Values	All Axial Levels Included
σ (integrated)	4.7%	4.7%
R.F. (integrated)	8.1%	8.1%
σ (nodal)	7.0%	9.0%
R.F. (nodal)	11.1%	12.7%

Question 18

If NSP selected the option to provide its own support for the process computer and generates its own data for this system, how will the change in uncertainty be accounted for in the safety limit?

Response

The plant computer calculations of bundle integral and nodal power distributions and local pin power distributions may be affected if NSP selects to support the GE Monicore system with the NSP physics methodology.

For monitoring and core surveillance, the power distribution parameters (APLHGR, LHGR, MCPR) will be compared to the safety limits such that power distribution parameter ≤ safety limit (APHLHGR, LHCR) or ≥ safety limit (MCPR). The power distribution parameters are the best estimate values calculated by the plant computer monitoring program.

If the option is chosen for NSP to provide support for the process computer, the uncertainty will be recalculated and the basis for this calculation will be included in the Reload Safety Evaluation for that cycle.

Question 19

Describe the fuel loadings for the cycles 7 through 10 cores which are included in the verification process of the NDH code. Provide information on fuel types, U^{235} - enrichment, gadolinia, water rods, etc. Are the fuel loadings of cycles 7 through 10 representative of cycle 14 and future cycles?

Fuel exposed in cycles 7 through 10 is described in Table 1. Ranges are given for the number of water rods per assembly and the number and enrichment of gadolinia rods per assembly. Also shown are the range of average bundle enrichments and pellet enrichments since all bundles are radially zoned. Reloads 6 through 9 were fabricated with natural uranium blankets at the top and bottom of the rods while reloads 2 through 5 were not. Nominal fuel rod dimensions have remained constant since the final reload for cycle 7, when small changes were made in the clad, pellet, and water rod dimensions. Table 2 shows the makeup of cycles 7 through 10 in terms of the cycle exposure and core loading. Cycles 7 through 10 include both high and low radial leakage core designs. Cycles 1 through 5 included fuel with a 7x7 lattice while later cycles were entirely 8x8.

Perturbations in core designs from cycles 5 thru 10 are greater than any we would anticipate in future cycles. The generic normalization factors are more sensitive to global factors such as high or low radial leakage core designs and less sensitive to local effects such as changes to fuel assembly designs, ie. enrichments, number of water rods, number of fuel pins, degree of moderation or number and enrichment of burnable poison rods. Cycle 12 has a control cell core and the statistics for the statepoints are as good or better than they are in the Topical. Therefore, we expect that the model will be applicable to all future designs. However, as we have stated elsewhere the nodal and integrated power distribution reliability factors will be calculated on the last three cycles of operation and updated in the Post Startup and Operation Report. This will ensure that any adverse trends in calculated to measured parameters will be detected at the earliest possible moment.

TABLE 1
RELOAD FUEL DESCRIPTION

	Cycles 7-10	Cycles 11-12
Number Water Rods/Assembly	1-5	in cycles 7-10 range
Number Gad Rods/Assembly	up to 7	in cycles 7-10 range
Gad Enrichment (w/o)	up to 4.0	in cycles 7-10 range
Bundle Average U^{235} Enrichment (w/o)	up to 2.84	up to 2.99
Pellet U^{235} Enrichment (w/o)	up to 3.8	up to 3.95

TABLE 2
CYCLES 7-12 DESCRIPTION

Cycle	Cycle Exposure	Core Loading
7	7901.8 MWD/MTU	88.4 MTU
8	6106.9	87.8
9	6625.9	87.0
10	6786.8	86.3
11	8184.6	86.5
12	8136*	86.5

* Predicted value

Response to NRC Questions on the NSP Reload Safety
Evaluation Methods for Monticello
NSPNAD-8608

Question 1

Does the DYNODE-B fuel rod gap heat transfer coefficient account for exposure and fuel temperature dependence and, if not, what error does this simplification introduce?

Response

The DYNODE-B model for the gap heat transfer coefficient allows for the effects of fuel temperature and exposure to be included. However, in the current methodology neither of these effects is modeled. Instead, a constant value of 1000 Btu/hr ft^2 °F is used, as is done in the REDY and ODYN analyses performed by General Electric (References 1 and 2). As the fuel vendor, General Electric has reported that this assumption conservatively bounds the actual predicted values of gap conductance. The error introduced by this assumption is, therefore, in the conservative direction. The DYNODE-B model for the gap heat transfer coefficient is described in Equation (10) of the DYNODE-B user's manual.

Reference 1 NEDS-20016, "Monticello Nuclear Generating Plant Second Reload License Submittal," General Electric Co., October 1973

Reference 2 NEDE-24011-P-A, "General Electric Standard Application for Reactor Fuel," General Electric Co., current revision 8, May 1986.

Question 2

What direct moderator heating fraction is used and is this value conservative for the transients to be analyzed (Table 4.1-1, MSIV closure, etc.)?

Response

For these benchmarks, a constant value of 0.02 is used for the direct moderator heating fraction in all transients, as was done in the corresponding ODYN and REDY analyses. This is a nominal value based on General Electric's calculations of bypass heating and non-fuel heating fractions for the reloads in question.

This value may change for future reloads. For licensing purposes, a conservatively small bounding value will be determined on the basis of fuel design, bundle and channel geometry, void fraction, and control fraction. This value will normally be provided by the fuel vendor.

Question 3

Comparisons have been presented for the DYNODE-B and the Nuclear Data Handling (NDH) System prediction of control rod worth and void reactivity. How do DYNODE-B and NDH compare with respect to Doppler reactivity?

Response

A comparison of the Doppler reactivities calculated with NDH and with DYNODE-B is shown below. The base case uses a core average fuel temperature of 917.6°F. The second case imposes a 50% increase in ΔT between the fuel and the moderator.

	k_{eff}	
	NDH	DNB
ΔT_{base}	1.0199	1.0199
(150% ΔT_{base})	1.0155	1.0155
Reactivity Change =	0.0044	0.0044

These results show that DYNODE-B and NDH Doppler feedbacks are equivalent, so that no additional uncertainty factor needs to be applied; i.e. $AF_{COLLAPSE}=0$.

Question 4

In the DYNODE-B/REDY comparisons, what REDY input was unknown and how was it determined? Was this input data adjusted to improve the DYNODE-B/REDY comparisons?

Response

The purpose of the code to code comparisons is to show that comparable results are produced by modeling identical transients, rather than by using identical input parameters. There has therefore never been a direct comparison made between the DYNODE-B and REDY inputs, nor is one necessary.

In general, only the input data published in the FSAR or USAR, or the cycle-specific parameters determined jointly by GE and NSP are known to have been used in the GE analyses. These include fuel geometry, scram and ECCS initiation setpoints, relief valve setpoints and capacities, bypass valve capacity, certain kinetics parameters, and the initial plant conditions for the transient.

The unknown input included such items as the modeling of the various controllers; main steam line geometry, friction factors, loss coefficients, and valve characteristics; scram curve and scram system delay; ECCS pump curves; RCP characteristic curves and drive motor data; reactor vessel geometric and fluid region modeling; reactor vessel pressure drop coefficients and inertias; and delay neutron modeling.

The DYNODE-B input decks were prepared on the basis of the Monticello FSAR, USAR, reload licensing submittals, plant drawings, equipment manuals, nuclear and thermal-hydraulics textbooks, engineering manuals, correspondence between NSP and General Electric, and several industry and General Electric publications. It is believed that much of the REDY input is taken from these same sources, and therefore much of the unknown REDY input should match that used in DYNODE-B.

The DYNODE-B input was based on the best available information and was not arbitrarily adjusted in order to improve the comparisons.

Question 5

The reduction in voids in the top of the core is expected to affect the axial albedo for the upper reflector. Has this effect been accounted for and, if not, what is the effect of this simplification on the DYNODE-B predictions?

Response

The axial albedos at the top and bottom of this core are assumed to be constant during the transient. These albedos are constant and equal to the corresponding NDH values for consistency with the 3-D reference models for the particular initial conditions. The axial albedo does not significantly affect the axial power distribution (and hence reactivity) for Monticello cores, since the top and bottom six inches of the fuel are natural U. The natural U regions act as buffers, reducing the importance of the fluid/structure reflector outside the active fuel region. In addition, the void fraction at the core exit (and hence in the reflector region) does not change significantly during the important portion of the transient, i.e., the period prior to the peak neutron power. The core exit void fraction changes by 2% to 3% during this period for the Monticello Cycle 11 benchmark cases. Thus, there is no effect of this modeling assumption.

Question 6

Are any codes that have not been approved by the NRC being used to provide input to DYNODE-B?

Response

No. All DYNODE-B input is prepared by hand except for those physics parameters generated according to the methods described in NSPNAD-8609.

Question 7

The recirculation loop modeling for both REDY and ODYN has been verified by comparison to recirculation pump trip tests. Has similar qualification been performed for DYNODE-B?

Response

This model has been benchmarked for the case of a single RCP trip transient using the startup test data taken on the Susquehanna Unit 1 as described in Reference 3. These qualifications demonstrate the adequacy of the model for analysis of RCP trip transients. The recirculation loop modeling in DYNODE-B has been qualified for recirculation pump trip tests for Monticello as described in Section 3.2.2.2.3 of NSPNAD8608.

Reference 3 R. C. Kern, "Qualification of a Loss-of-Recirculation Flow Model for Jet-Pump BWR's," Trans. Am. Nuc. Soc., 54, 241 (1987).

Question 8

What is the direction of conservatism for each input parameter, for which a conservative uncertainty allowance will be included, for the transients to be analyzed (Table 4.1-1., MSIV closure, etc.)?

Response

The attached Table 1 shows the direction of conservatism for each input parameter to ensure each transient on Table 4.1-1 is conservative. The fuel misloading error is not done using the DYNODE-B code, as is described in the response to question 20. The control rod worth, which is negative, is the scram worth for all transients except for the control rod withdrawal error transient, in which it is the worth of the rod being withdrawn. Power distribution includes LHGR, MAPLHGR, and bundle power. As an example, for the loss of feedwater heating transient, Table 1 would be read as follows: The power distribution has a "+"; therefore the reliability factor will be applied in a direction to increase the power distribution value. The void coefficient has a "-"; therefore the reliability factor will be applied in a direction to obtain the most negative coefficient. This will increase the feedback effect. The Doppler coefficient has a "+"; therefore the reliability factor will be applied in a direction to obtain the least negative coefficient. This will decrease the feedback effect. The control rod worth has a "+"; therefore the reliability factor will be applied in a direction to obtain the least negative scram worth. This will reduce the scram reactivity. The kinetic parameters have a "-"; therefore the reliability factor will be applied in a direction to decrease the kinetics parameters.

Question 9

Are the void models in DYNODE-B and NDH identical? Are the values for the void concentration parameter, C_o, and drift velocity, V_{gj}, used in the NDH calculations the same as used in DYNODE-B? If not, what is the effect of this inconsistency on the K_∞ and M^2 calculated by DYNODE-B and on the DYNODE-B results?

Response

The void models in DYNODE-B and NDH are not identical, and the values of the void concentration parameter and drift velocities are different. This inconsistency is taken into account in the method used to compute the void reactivity feedback parameters which are input to DYNODE-B in the following manner. The NDH model is perturbed from the reference (initial) condition to produce a change in the local void fractions and hence k_∞ and M^2. Normally this perturbation is introduced by changing the subcooling (via a pressure change) and maintaining all other thermal hydraulic parameters constant. The DYNODE-B model is perturbed in an identical manner to generate the corresponding local void fraction changes. The changes in k_∞ and M^2 obtained from NDH are then correlated to the changes in the DYNODE-B void fraction changes. Thus, the two models predict the same change in reactivity for the same change in the boundary thermal hydraulics conditions, so that the overall results of the two models are self-consistent.

Question 10

List all significant code and modeling differences between DYNODE-B, and REDY and ODYN and provide estimates of the effect of these differences on the DYNODE-B predictions when it cannot be demonstrated that the differences provide improved modeling or more conservative results.

Response

The significant code and modeling differences between DYNODE-B and REDY and ODYN codes are discussed in Sections 3.2.1.1 and 2.3, respectively, and are summarized below.

REDY

Dynamic Void Effects:

REDY: second order sweep model
DYNODE-B: profile-fit non-equilibrium flow quality void model

The profile-fit model in DYNODE-B is an improved model.

Decay Heat:

REDY: Stehn-Clancy Correlation (1965)
DYNODE-B: 1971 ANS Correlation

The DYNODE-B correlation offers improved modeling over the REDY correlation.

Cladding Surface Heat Transfer Coefficient:

REDY: Constant value
DYNODE-B: Thom correlation

The Thom correlation accounts for the effects of changing fluid and heat flux conditions, and therefore provides improved modeling.

ODYN

Core neutronics:

ODYN: one-group diffusion theory
DYNODE-B: total fission source nodal equations

The DYNODE-B nodal formulation can be derived from the one-group equations; these models are equivalent.

Decay Heat:

ODYN: exponential decay model
DYNODE-B: 1971 ANS correlation

The 1971 ANS Standard is a more sophisticated model for decay heat calculation.

3D to 1D radial collapsing:

The collapsing procedure for DYNODE-B is more rigorous than that used for ODYN, because the 3D and 1D neutronic models are identical in NDH and DYNODE-B, providing improved modeling by ensuring self-consistency between the 3D and 1D formulations.

Steam Line:

ODYN: single-phase 1D nodal representation
DYNODE-B: 1D conservation of mass, energy, momentum, and state - Method of Characteristic (MOC) Solution

The MOC methodology is more rigorous and does not assume that the steam is isentropic. This therefore represents improved modeling.

Reactor Vessel Pressure Distribution:

ODYN: explicit calculation of pressures at reactor inlet and reactor vessel dome
DYNODE-B: explicit calculation of dome pressure; reactor pressure based on transport delay between dome and core outlet.

Because the changes in pressure in the vessel dome during an overpressurization event are larger than those in the core, the DYNODE-B method conservatively overpredicts the core pressure.

These are the only significant differences known to exist between DYNODE-B and REDY and ODYN. Unknown differences may exist, but since the effects of any such differences are included in the benchmarks, and since those benchmarks show good agreement with REDY and ODYN, any unknown differences have little effect on the overall results.

Thus, for each of the modeling differences, DYNODE-B provides either improved or more conservative modeling.

Question 11

Reference 7 recommends the mechanistic rather than the profile-fit void model for transient applications. Since DYNODE-B allows both the mechanistic and profile-fit void model, what is the basis for the selection of the profile-fit model?

Response

The profile-fit model was selected on the basis of the results described in Reference 4. The major conclusion of that work is that the profile-fit model produced larger void fraction changes during over-pressurization events and hence resulted in a more conservative result. It has since been discovered that an error existed in the Reference 4 analysis, rendering it inconclusive. Nevertheless, the model qualification presented in NSPNAD-8608 has demonstrated the adequacy of the use of the profile-fit model for transient applications for Monticello based on comparisons to test data and other licensing calculations.

Reference 4 R. C. Kern, et. al. "Qualification of an Advanced BWR Transient Model for Pressurization Transients," Trans. Am. Nuc. Soc. 39, 629 (1981).

Question 12

The DYNODE-B definition of the volumetric flow fraction, β, the concentration parameter, C_o, and the drift velocity, V_{gj}, involve arbitrary constants (viz., C_{00}, C_{01}, b_1, β_1, V_{gj1}, V_{gj2}). How are these constants determined and what uncertainty is introduced into the DYNODE-B calculations by the selection of these constants? Also, the definition of β in DYNODE-B appears to be in error.

Response

The constants used to define the void concentration parameters, the drift velocity, and β are given in Reference 5, which are the DYNODE-B code default values. The uncertainties associated with these values are included in the total model uncertainty, which the benchmarks show to be conservative. The defining equation for β in the DYNODE-B user manual is incorrect, but the coding uses the correct definition. The user's manual will be corrected to read:

$$\langle\beta\rangle = \frac{\langle x\rangle\beta_1}{\langle x\rangle+(\rho_g/\rho_1)\,(1-\langle x\rangle)} \qquad (36)$$

Reference 5 R. T. Lahey, Jr. and F. J. Moody, "The Thermal-Hydraulics of a Boiling Water Nuclear Reactor," ANS Monograph Series on Nuclear Science and Technology, 1977.

Question 13

Describe in detail the core thermal-hydraulic model used to determine the axial pressure, void, flow and enthalpy distributions. Have the resulting equations been tested for numerical stability?

Response

The profile-fit non-equilibrium flow quality model used in this analysis is described in detail in section 3.3.2 of the DYNODE-B manual. The axial void distribution is determined by computing the void fractions at the ends of each axial node, and the node average void fraction is obtained by assuming a linear distribution within each node. For the first node in which voids appear, the void fraction is assumed to be linear between the point of bubble detachment and the top end of the node.

Because the pressure drop across the core is relatively small, and because in practice most of the drop occurs across the bottom core plate rather than in the active fuel region, the actual pressure variation from node to node is small enough to be of little impact in determining conditions in each node when compared to the much larger effect of such changing variables as fluid enthalpy. Therefore, in performing core calculations, the core pressure is assumed to be axially uniform.

The axial flow distribution is determined by the conservation of mass. The enthalpy distribution is determined by simultaneously solving the equations of conservation of mass and energy (refer to Eqn (15) in the DYNODE-B manual).

These equations are solved using the Runge-Kutta-Merson method as referenced in the manual. Numerical stability is ensured by choosing the input parameters such that the code selects adequately small time steps which are much less than the Courant limit.

Question 14

In the calculation of steam dome pressure, what uncertainty is introduced by the use of the "steam-dome pressure model" rather than the "non-equilibrium steam-dome pressure model"?

Response

The model qualifications presented in NSPNAD-8608 demonstrate that the steam-dome pressure model used in the analysis consistently produces conservative results. It is therefore unnecessary to apply uncertainties due to the choice of pressure model.

Question 15

In the static flow distribution calculation, how is the bypass flow fraction determined and does it vary during the transient?

Response

The initial bypass flow fraction is an input parameter. Its value is chosen to be identical to the value used in NDH for the core physics calculations. During initialization, DYNODE-B calculates the corresponding bypass pressure drop coefficient in order to establish the desired bypass flow fraction at initial, steady-state conditions. The bypass flow then varies during the course of the transient according to the equations of conservation of momentum.

Question 16

How are the feedwater flow, recirculation flow, power level, turbine bypass and stop valve controller lead-lag, lag and controller constants determined and do they change for each cycle?

Response

The lead, lag, and controller constants used in modeling the various controllers represented in DYNODE-B are based on references 7,8, and 9. Other controller data is assembled from the Monticello Operations Manual, the FSAR, and correspondence between NSP and GE. This data is not cycle-specific and would normally only be altered if the controllers themselves were modified.

Reference 7 NEDC-10069, "Monticello Nuclear Power Station Plant Transient Design Analysis Report," General Electric Company, July 1969.

Reference 8 NEDO-10563, "Monticello Unit No. 1 Startup Test Results," General Electric Company, April 1972.

Reference 9 NEDO-10802, "Analyical Methods of Plant Transient Evaluations for the General Electric BWR," General Electric Company, February 1973.

Question 17

The flux, ϕ, rather than the source, $S=\nu\Sigma_f\phi$, satisfies the standard time-dependent diffusion equation. Has the additional term $\phi\partial_t(\nu\Sigma_f)$ been accounted for in the DYNODE-B source equations and, if not, what error is introduced by this approximation?

Response

The derivation of the time-dependent source equation used in DYNODE-B from the standard diffusion equation results in the left hand side (LHS) of Equation 80 of the user's manual as:

$$LHS = \frac{1}{v}\partial_t\phi$$

Multiplying the numerator and denominator by the initial value of $\nu\Sigma_f$ yields:

$$LHS = \frac{1}{\nu\nu\Sigma_f(0)} \nu\Sigma_f(0)\, \partial_t \phi$$

$$= \ell_0\, \partial_t\, (\nu\Sigma_f(0)\phi) \approx \ell_0\, \partial_t S$$

Since DYNODE-B uses the initial value for ℓ and assumes it to be constant, it is necessary to explicitly omit the $\phi\partial_t(\nu\Sigma_f)$ term for consistency. This formulation introduces only a small error, since the neglected terms are relatively small for events which result in large neutron flux changes due to significant reactivity changes. In these cases, the major changes in the source are due to changes in flux rather than in $\nu\Sigma_f$.

Question 18

What is the mechanism responsible for the underprediction of the scram curves (Figure 3.1-4) and can this result in a non-conservative overprediction for other static and transient states?

Response

The differences in scram curves between NDH and DYNODE-B arise from the process of collapsing the 3-D neutronics parameters of NDH to the 1-D parameters used in DYNODE-B. It is expected that the direction of these differences will vary, causing the DYNODE-B curve to be non-conservative for some cases (as in Figure 3.1-4) and conservative in others. Because of this, the results of each case are examined individually; when an overprediction occurs, the 1-D scram reactivity parameters which are derived from the collapsing procedure must be corrected so as to produce conservative results. The corrected parameters are then used in the licensing analysis.

It should be noted that there is virtually no difference in the DYNODE-B and NDH scram reactivities for the first two nodes (approximately one foot) of control rod insertion in Figure 3.1-4. This portion of the scram curve is the most important region, since the initial negative reactivity insertion in this period causes the neutron power to turn around.

Question 19

How do the DYNODE-B and ODYN peak powers in the load rejection, feedwater controller failure and MSIV closure transients of Figure 3.2-93, 3.2-100 and 3.2-107, respectively, compare? Are these differences due to DYNODE-B and ODYN modeling differences and, if so, why should they not be considered as a measure of the uncertainty in performing transient analyses of Monticello reloads?

Response

The figures provided by the vendor which document the results of the ODYN analyses do not show values beyond those presented in Figures 3.2-93, -100, and -107. Thus, it is not possible to compare the peak powers between DYNODE-B and ODYN. Differences in peak power predictions are due to both modeling and input differences. Because of the extremely high slope of the power spike during these transients, the predicted peak value is highly sensitive to any changes which affect the time at which the peak occurs; thus, meaninglessly small input changes can produce large changes in peak power.

However, the peak power is of less importance than the integral under the power curve, since this latter value determines the energy deposition in the fuel and hence the heat flux and ΔCPR. Because the power spike is quite narrow, the area is relatively insensitive to the peak value, and is not unduly sensitive to minor changes. Comparisons of the heat flux curves indicate that DYNODE-B does yield reasonable agreement with ODYN for the transient heat flux response. Those differences which are attributable to void and scram reactivity parameters used in the two different models are discussed in the respective sections of NSPNAD-8608. No additional uncertainties are required for performing transient analyses of Monticello reloads because of these differences, since the physics parameters will be treated in a conservative manner.

Question 20

Describe how DYNODE-B is used in the calculation of the fuel misloading error and how the reactivity input is determined. How are radial redistribution effects accounted for?

Response

DYNODE-B is not used in the calculation of the fuel misloading error. This event is evaluated with the NDH and CASMO computer codes which are described in report NSPNAD-8609. For the mis-oriented or rotated bundle, CASMO will be run to determine the increase in the fuel type local peaking factor. For the mis-located bundle, NDH will be run to determine the effect on the core power distribution. There is an error on Table 4.1-1 stating that the fuel loading error is evaluated using point kinetics. Table 4.1-1 should indicate that three-dimensional steady state methods are to be used.

Question 21

In the application of DYNODE-B to the control rod withdrawal event, what error is introduced by not including the radial flux distribution changes explicitly in the calculation? Does the non-equilibrium model include the time dependent mass and energy balance for the (1) riser and dome steam (2) riser liquid (3) dome liquid and (4) the entrapped steam. If not, what error is introduced by this approximation?

Response

The control rod withdrawal error event is analyzed with the 3-D nodal code, NDH, which calculates the effects of radial and axial flux redistribution. DYNODE-B may be used to determine the transient pressure response to this event, so that the influence of the changing pressure may be included in the NDH calculations if desired.

The non-equilibrium steam dome pressure model does include the time-dependent mass and energy balance for each of these four thermodynamic "compartments".

Question 22

Explain any differences between the Table 4.2-1 initial conditions and input parameters and the corresponding values and conditions assumed in the ODYN analyses. What effect do these difference have on the DYNODE-B predictions of ΔCPR, peak pressure and decay ratio for the transients to be analyzed?

Response

The initial conditions listed in Table 4.2-1 are those used in the DYNODE-B comparisons to ODYN and REDY; these will not necessarily be unchanged for future reload analyses. For clarification, Table 4.2-1 will be retitled in future revisions to "Initial Conditions and Input Parameters for DYNODE-B Comparisons to ODYN and REDY Reload Safety Evaluations of Monticello."

The only known differences between these conditions and those used in the ODYN analysis are as follow:

	DYNODE-B	ODYN	Comments
Core inlet enthalpy (Btu/lbm)	524.7	524.2	Corresponds to rated steam flow. No other significant impact is expected.
Turbine Control Valve closure (msec)	246	300	The TCV closure in DYNODE-B is completed 54 msec sooner than in ODYN, making the resulting pressure spike slightly more severe.
Initial Vessel Water Level-Sensed (inches)	36.9	36.5	Table 4.2-1 contains a typographical error: the initial DYNODE-B water level is 30 inches, which corresponds to a sensed level of 36.9 inches. No significant impact on the transient results due to this difference is expected.

The known differences in initial conditions are slight, and are expected to have no noticeable effect on the transient results.

Question 23

How are the uncertainties in the bundle power and relative inlet flow due to differences in the static and transient radial power and flow distributions accounted for in the determination of ΔCPR?

Response

In determining ΔCPR for each transient, a sequence of differing bundle powers and flows are analyzed in order to identify those combinations which yield a transient MCPR equal to the safety limit. The ICPR's of these bundles are then compared to identify the highest among them; this value represents the highest ICPR which can produce a transient MCPR equal to the safety limit, and thus defines ΔCPR for the event.

Because this method of determining ΔCPR identifies the largest ΔCPR regardless of radial variations in power and flow, no uncertainty arises from those variations.

Question 24

What range of operating state variables, including power level, flow, inlet subcooling, control rod pattern and exposure, were used to determine the collapsing factor (AF)? Demonstrate that this set of states is sufficient in view of the wide range of intended applications (Table 4.1-1, MSIV closure, etc.). What is the Doppler reactivity collapsing factor (AF) and how is this uncertainty accounted for?

Response

The ranges of the operating state variables which are used to generate the feedback parameters are determined for each specific transient which is being analyzed and are sufficient to cover the ranges over which these variables change during the important portion of the event; i.e., up to the time of the peak neutron power. The manner in which these ranges are covered is also consistent with the manner in which the variables change during the event. As an example, consider an overpressurization transient in which void collapse occurs. For this case, the void reactivity parameters are calculated using the NDH and DYNODE-B models as described in the answer to Question 9 by increasing the core pressure and maintaining the inlet enthalpy. The core pressure change is at least as large as the value which occurs at the time of the peak neutron power. The axial collapsing factor for the void reactivity is determined for this same specific set of conditions and calculations. Thus, AF is determined in an appropriate manner for each specific case and over the appropriate range for the feedback parameters. The AF factors for Doppler and scram are determined in a similar manner. Because these factors are determined in a conservative fashion, no uncertainty due to the collapsing process need be considered.

Question 25

Describe in detail the method used to determine the DYNODE-B equivalent one-dimensional k_∞, M^2, g_v and albedos from the three-dimensional NDH solutions. Describe the perturbed states used in this determination in terms of core power, flow, inlet subcooling, pressure and exposure.

Demonstrate that these selected perturbed states provide an adequate representation of the transient states encountered in the events to be analyzed (Table 4.1-1, MSIV closure, etc.). How are the k_∞, M^2, g_v and albedos determined for the control rod insertion/withdrawal events?

Response

The method for determining the DYNODE-B equivalent one-dimensional k_∞, M^2, g_v and albedos from the three-dimensional NDH solutions is described in detail in Reference 6. This reference describes the technique for both the initial conditions and the feedback parameters. The method for determining the perturbed states is also described in the sections which deal with generation of the feedback parameters with the following changes:

1. Fuel Temperature
   In NDH the local reactivity changes are represented by the equation in section 2.2.2.2 of the NDH manual. The change in the NDH cases is done by changing the input value to B20 and not PR as stated in Reference 6. The effect is exactly the same.

2. Delayed Neutrons
   The BELLEROPHON program is not used as discussed in Reference 6. The delayed neutron parameters are calculated as shown in the NDH manual setion 2.2.5.

3. Source to Power Ratio
   The equation to calculate the source to power ratio is shown in section 2.2.3 of the NDH manual.

An example of this is described briefly in the answer to Question 24, which also notes that the treatment is adequate. Reference 6 also covers the cases in which control rods are either inserted or withdrawn.

Reference 6 R. C. Kern, "Methods and Guidelines for Obtaining One-Dimensional Nodal Constants for DYNODE-B from Three-Dimensional Nodal Calculations," NAI 82-26, Rev. 1, May 20, 1982.

Question 26

The ODYN model has had difficulty in prediting core inlet flow oscillations above 5 hz. If DYNODE-B will be required to analyze oscillations above this frequency, demonstrate that DYNODE-B does not have the same difficulty.

Response

The ability of DYNODE-B to predict high frequency oscillations in the core inlet flow was tested by imposing high frequency variations as input to the flow equation, using both large and small perturbations. This was accomplished by forcing a 5 Hz oscillation in recirculation pump speed, first with the amplitude varying between 50% and 150% of initial speed, and then between 90% and 110%. Both cases were then repeated using a 10 Hz oscillation.

In all cases, DYNODE-B produces stable results for all system parameters, such as power, flow, and pressure (see Figures 26-1 and 26-2). It is therefore unnecessary to place restrictions on the dynamic flow model even for high frequency responses.

Question 27

The qualification data base provided to demonstrate the accuracy of the DYNODE-B code (e.g., Tables 4.4-1, 4.4-2 and 4.4-3) is insufficient in the number and quality of the comparisons to allow a reliable estimate of the code uncertainty. For example, the Peach Bottom turbine trip calculations were normalized to insure that DYNODE-B reproduced the measured peak and integrated power, and the comparison for the Monticello turbine trip startup

test includes a large (-300%) DYNODE-B/measurement transient power discrepancy. A detailed code uncertainty analysis is therefore required to insure there is sufficient margin to the thermal-hydraulic design basis and the reactor coolant pressure boundary limit.

Provide a listing of the important sources of uncertainty in the DYNODE-B predictions required for the intended reload analyses. Consideration should be given to factors such as: void coefficient, controller set points, jet pump loss coefficients, scram reactivity, void model, separator model, steam line model, neutronics collapsing, etc. Estimate the 95% probability limits for these uncertainties, and determine the corresponding ΔCPR/ICPR for each uncertainly for the turbine trip without bypass transient. Determine the corresponding Δ-pressure (%) for each of these uncertainties for the MSIV closure event with position switch scram failure. Also, provide an estimate of the corresponding uncertainty in the calculated decay ratio.

Response

Although the data base used to qualify the accuracy of the DYNODE-B code is small, NSP believes that it is sufficient to demonstrate that the code uncertainties (excluding the neutronic model) are consistent and conservative. The Peach Bottom turbine trip calculations yielded a consistent +10% in ΔCPR relative to the "measured" values for the cases in which the energy deposition in the fuel matched the test results. Thus, the T+H code uncertainties are uniformly consistent and conservative. The reason that no additional code uncertainties need be considered is that the neutronic model will be used in a conservative bounding manner in that the conservative bias and reliability factors will be applied to each of the reactivity feedback parameters as described in Section 4.2 of NSPNAD-8608. These are the most significant parameters in the model which affect the transient ΔCPR, peak reactor vessel pressure increase, and decay ratio.

Question 28

What mesh is used in the MOC representation of the steam line and does this satisfy the stability criteria? The steam line flow in Figure 3.2-96 does not exhibit the same behavior as the ODYN prediction. What is causing this difference?

Response

The mesh used in the Monticello DYNODE-B steam line MOC model varies between 22.3 and 29.4 feet. This mesh representation is stable, since the normal time step size for the steam line solution is 0.001 sec for overpressurization events and the speed of sound in steam is about 1500 ft/sec. Thus, the Courant limit is not exceeded. The steam line flow differences between DYNODE-B and ODYN as seen in Figure 3.2-96 are attributable to model differences as noted in Section 2.3.2 of NSPNAD-8608 and in the response to question 10. The volume-junction representation used in ODYN is more susceptible to instabilities relative to the MOC method, provided the latter model does not exceed the Courant limit. As noted in Figure 3.2-96, the DYNODE-B steam line flow settles to the new asymptotic value more quickly and smoothly compared to the ODYN result.

Question 29

How does the DYNODE-B decay heat precursors model compare with more recent revisions of this standard (e.g., the ANS standard of September, 1978)?

Response

For any given case, the later standard for decay heat calculations, ANSI/ANS-5.1-1979, may yield a decay heat value which is either greater or smaller than the value derived using the 1971 ANS-5.1 Draft standard, depending on the specific conditions being analyzed; it therefore cannot be said that either method is always the more conservative. However, the uncertainties associated with the 1971 methods are much larger than with the 1979 standard; as a result, when the uncertainties are applied, the 1971 methods consistently produce a more conservative prediction of decay heat. For all licensing calculations, those uncertainties are included in the DYNODE-B model, thereby ensuring a conservative decay heat calculation.

TABLE 1
Direction of Application of Reliability Factors

Transient	Power Distribution	Void Coefficient	Doppler Coefficient	Control Rod Worth	(β, ℓ^*) Kinetic Parameters
1. Loss of Feedwater Heating	+	-	+	+	-
2. Feedwater Controller Failure-Maximum Demand	+	-	+	+	-
3. Pressure Regulator Failure-Open	+	+	-	+	+
4. Pressure Regulator Failure-Closed	+	-	+	+	-
5. Generator Load Rejection	+	-	+	+	-
6. Turbine Trip	+	-	+	+	-
7. MSIV Closure	+	-	+	+	-
8. Loss of Condenser Vacuum	+	-	+	+	-
9. Loss of AC Power Transformer	+	+	-	+	+
10. Loss of Auxiliary Power	+	+	-	+	
11. Loss of Feedwater Flow	+	+	-	+	+
12. Recirculation Pump Trip	+	+	-	NU	+
13. Recirculation Flow Control Failure-Decreasing Flow	+	+	-	NU	+
14. Abnormal Startup of Idle Recirculation Pump	+	-	+	+	-
15. Recirculation Flow Control Failure-Increasing Flow	+	-	+	+	-
16. Control Rod Withdrawal	+	+	+	-	-
17. Inadvertent HPCIS or RCICS Activation	+	-	+	+	-
18. Inadvertent Safety/Relief Valve Opening	+	+	-	+	+

\+ Indicates an increase in the value or the least negative value

\- Indicates a decrease in the value or the most negative value

NU Indicates the parameter is Not Used.

MONTI CYC11 BOC BEST ESTIMATE
5HZ RCP SPEED OSCILLATION 150%-50%

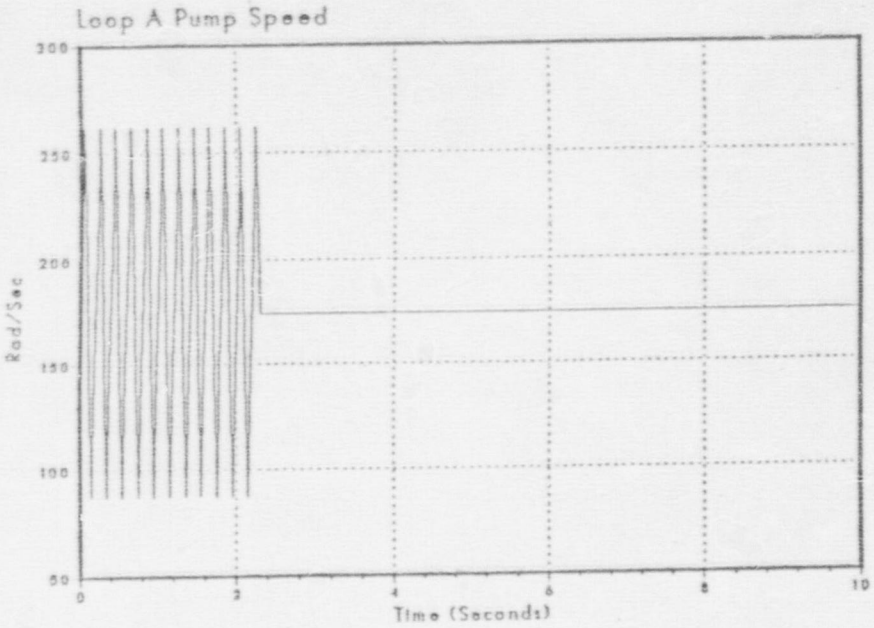

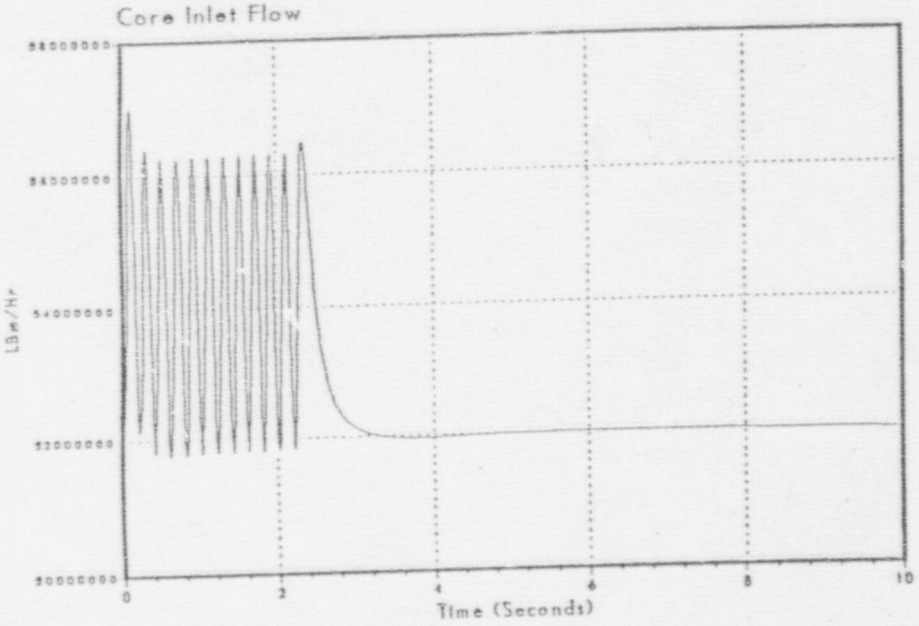

MONTI CYC11 BOC BEST ESTIMATE
5HZ RCP OSCIL 110%-90%

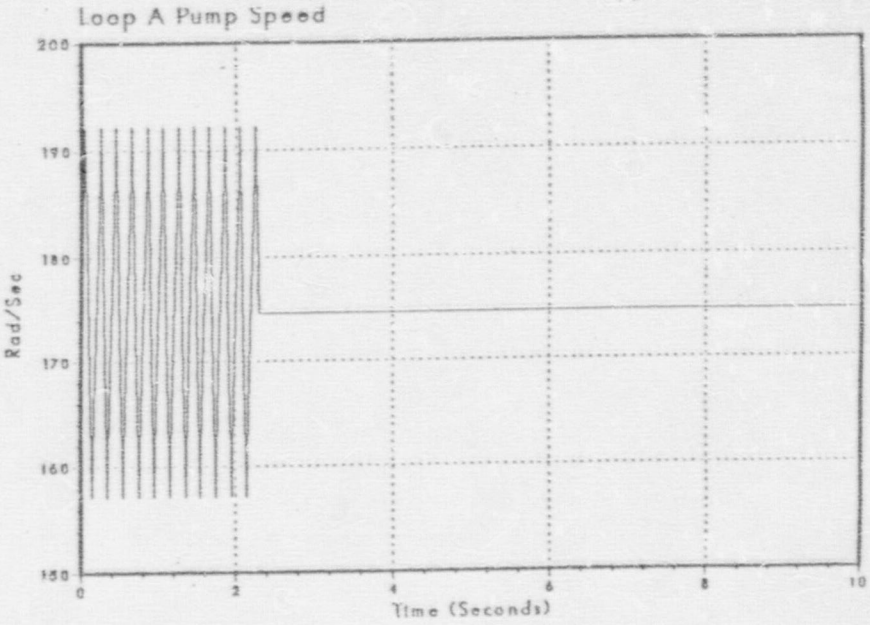

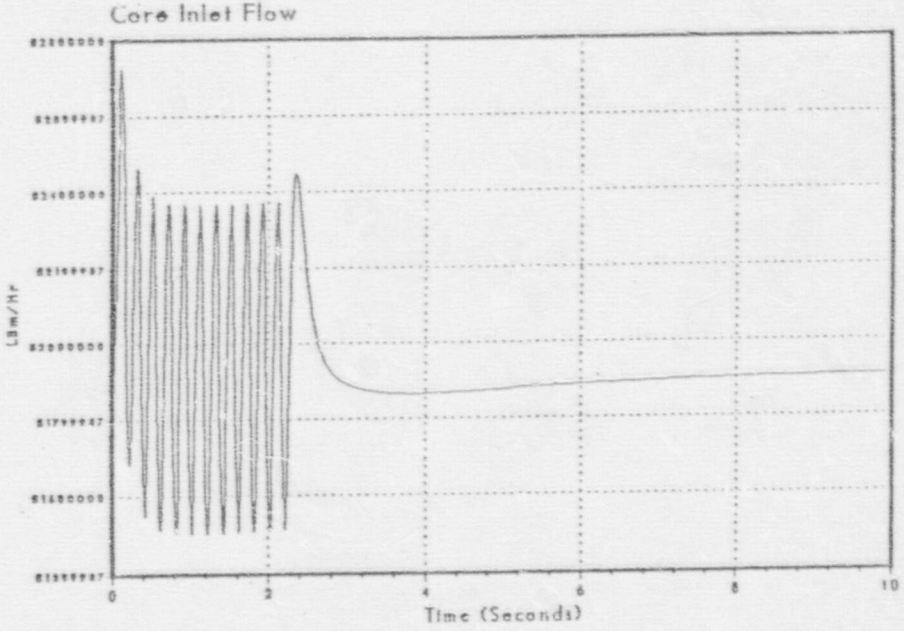

Figure 26-1

MONTI CYC11 BOC BEST ESTIMATE
10HZ RCP SPEED OSCILLATION 150%-50%

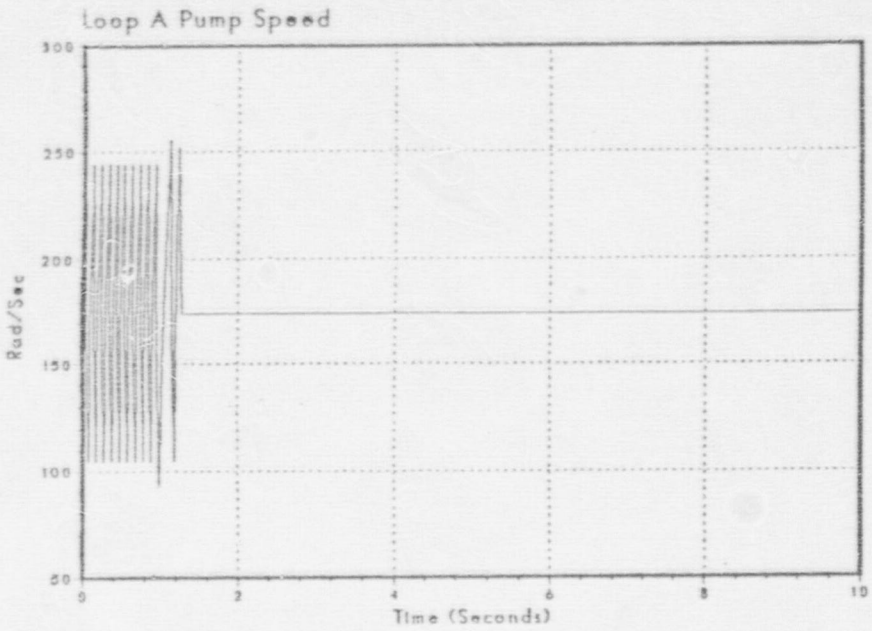

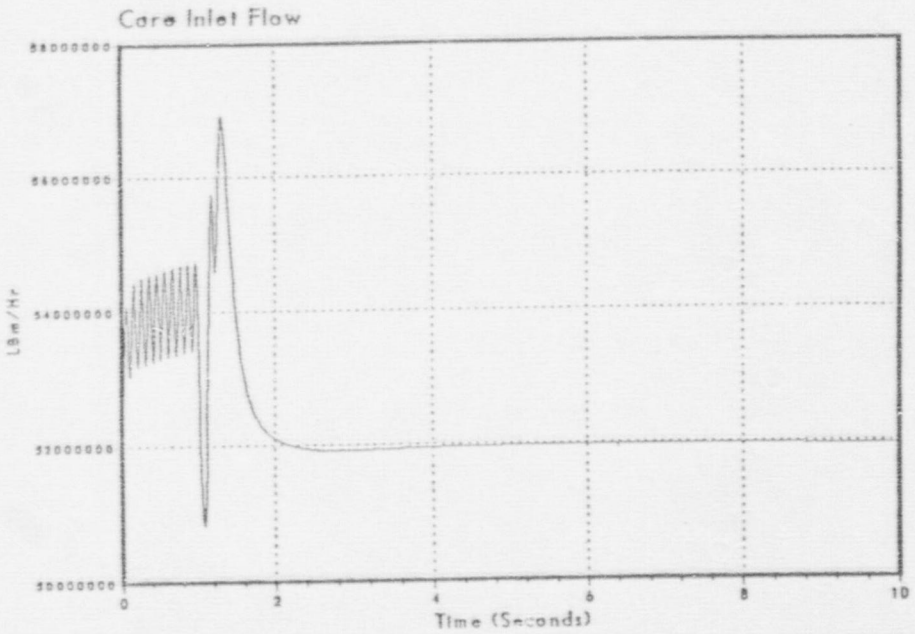

MONTI CYC11 BOC BEST ESTIMATE
10HZ RCP OSCILLATION 110%-90%

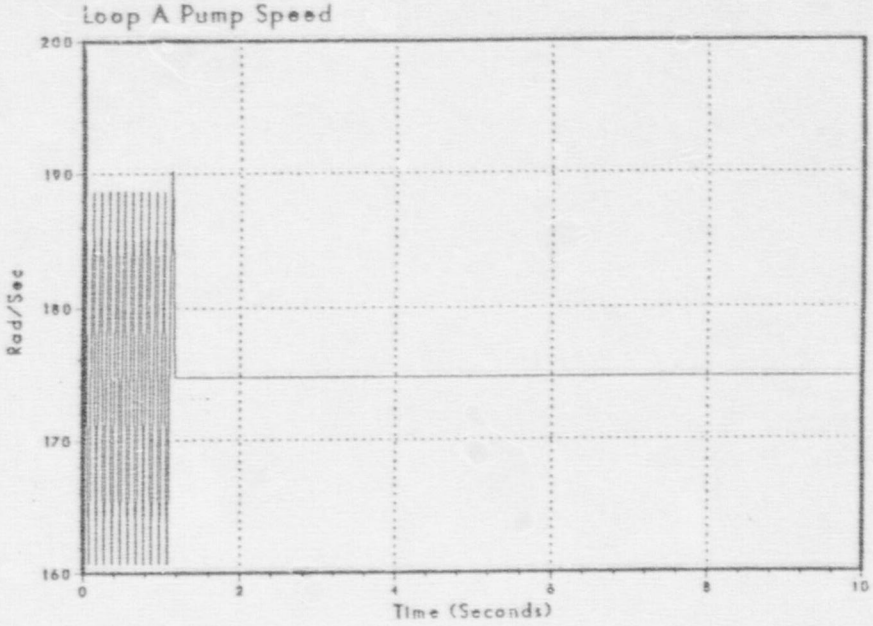

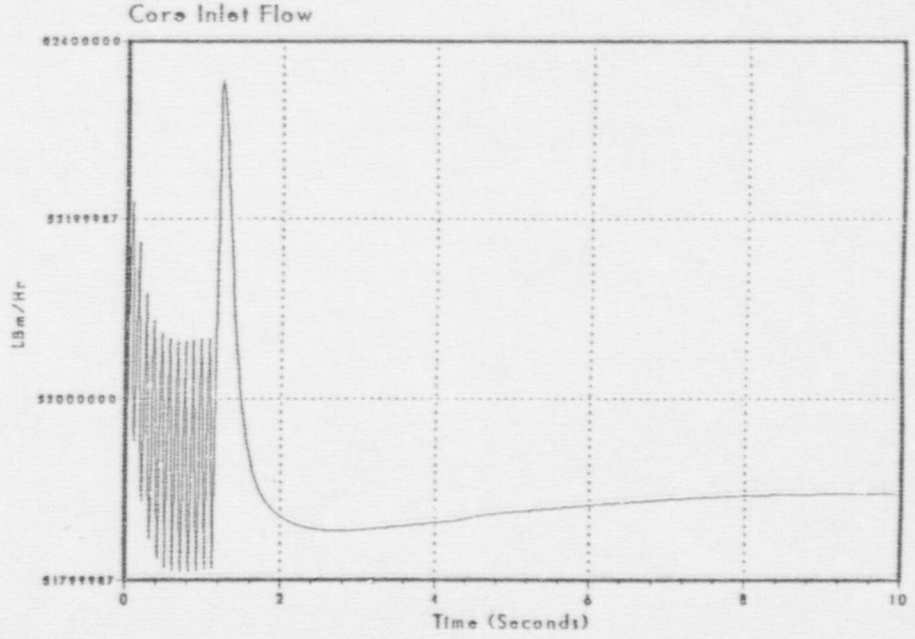

Figure 26-2